ACADEMIC PRESS

Available online at www.sciencedirect.com

SCIENCE DIRECT®

Journal of Magnetic Resonance 159 (2002) 161–166

JMR Journal of Magnetic Resonance

www.academicpress.com

An active resonator system for CW-ESR measurement operating at 700 MHz

Toshiyuki Sato,[a] Hidekatsu Yokoyama,[b,*] Hiroaki Ohya,[b] and Hitoshi Kamada[b]

[a] *Yamagata Research Institute of Technology, Yamagata 990-2473, Japan*

[b] *Institute for Life Support Technology, Yamagata Public Corporation for Development of Industry, 2-2-1 Matsuei, Yamagata 990-2473, Japan*

Received 23 May 2002; revised 3 September 2002

Abstract

An active resonator system operating at 700 MHz, which can attain a high Q for CW-ESR measurements of a high loss sample, was developed. This system consisted of a loop-gap resonator (LGR), a receiver coil, an excitation coil, and a phase tunable amplifier. A part of the RF power at the LGR was picked up by the receiver coil, amplified, and irradiated to the LGR again by the excitation coil, which made up a feedback circuit. Because the feedback circuit provided the energy that canceled the loss in the resonator, the Q of the active resonator system increased. When a sample tube (inner diameter, 20 mm; axial length, 31 mm) containing a nitroxide radical and physiological saline solution was placed in the resonator, the Q could be varied from 55 to 4000. It was possible to obtain a Q of the active resonator system with sample that was higher than that of the value of the LGR without a sample in a no-feedback condition. The ESR signal intensity increased up to 7 times with the increase in Q. The sensitivity increased up to 50%, which was a much smaller advance than that of the Q, because the noise level also increased with the increase in signal intensity.

Keywords: ESR; EPR; Resonator; Feedback; RF

1. Introduction

In CW-ESR measurements, a resonator operating at the ESR frequency is an indispensable component. The alternating magnetic field, B_1, is applied to the sample efficiently by the resonator and the absorption of RF power caused by the ESR is emphasized as the change of reflected power. The filling factor and homogeneity of B_1 are important factors of the resonator, especially for in vivo ESR measurements. The loop-gap resonator (LGR) is known for its large filling factor and homogeneity [1,2]. However, when the LGR is loaded by a biological sample at a large filling factor, the Q-value drops considerably, which decreases the ESR signal intensity. The drop in Q also necessitates re-adjusting the coupling between the resonator and the transmission line. The Q of the resonator is defined by,

$$Q = 2\pi W_S / W_D, \tag{1}$$

where W_S is the energy stored in the resonator and W_D is the energy dissipated per RF cycle in the resonator. Efforts have been made to increase the Q under sample-loaded conditions by reducing W_D. A bridge shielded LGR [3,4] or multi-layered resonator [5] has been proposed to reduce the electric field in the sample space, which reduces the dielectric loss in an aqueous sample. However, it is difficult to eliminate the electric field completely in the sample space. Further, the eddy currents in the sample induced by B_1 also waste energy.

If one externally supplies energy by using some active device to cancel the loss in the resonator (i.e., W_D), the drop in Q caused by the sample loading could be reduced. In this study, an "active resonator system," which consisted of an LGR, a receiver coil, an excitation coil, and a phase tunable amplifier, was fabricated. A part of the RF power from the LGR was picked up by the receiver coil, amplified, and irradiated to the LGR

* Corresponding author. Fax: +81-23-647-3149.
E-mail address: yokohide@fmu.ac.jp (H. Yokoyama).

1090-7807/02/$ - see front matter © 2002 Elsevier Science (USA). All rights reserved.
PII: S1090-7807(02)00017-4

again by the excitation coil. By using this system, the Q and ESR signal intensity increased.

2. Results

2.1. Active resonator system

A block diagram of the active resonator system is shown in Fig. 1. The resonator is an LGR (two-gap type; center frequency, 703 MHz without sample; inner diameter, 40 mm; axial length, 10 mm). The coupling coil is a single-turn coil (diameter, 40 mm; copper wire, 3 mm in diameter), where the magnetic coupling can be adjusted by moving the coupling coil along the axis of the LGR. The distance between the coupling coil and the LGR is referred to here as the "coupling distance." The excitation and receiver coils are single-turn elliptical coils (long diameter, 23 mm; short diameter, 15 mm; copper wire, 1 mm in diameter). The excitation and receiver coils were tilted at different angles to the LGR to reduce the direct coupling between them. The resonator, coupling, receiver and excitation coils, and a pair of modulation coils were put in a shield case to prevent the radiation of RF power and noise penetration.

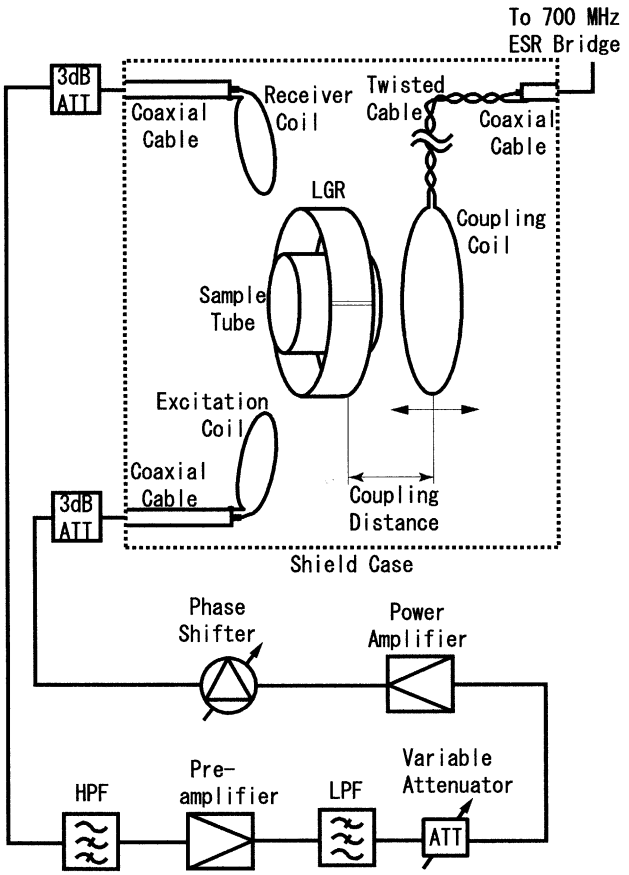

Fig. 1. Block diagram of an active resonator system, which consisted of an LGR, a receiver coil, an excitation coil, and a phase tunable amplifier. A part of the RF power at the LGR was picked up by the receiver coil, amplified, and irradiated to the LGR by the excitation coil, which was built into a feedback circuit. The phase tunable amplifier, which amplifies the RF power and controls the phase, is constructed from a high-pass filter, pre-amplifier, low-pass filter, variable attenuator, power amplifier, and phase shifter. To suppress standing waves in the transmission lines, −3 dB fixed attenuators were used.

A photograph of the LGR and the coils in the shield case is shown in Fig. 2. The phase tunable amplifier, which amplifies the RF power from the receiver coil and allows the phase to be adjusted, consists of a high-pass filter (SHP-300, Mini Circuit, NY; cutoff frequency, 300 MHz), a pre-amplifier (ZFL-1000LN, Mini Circuit; frequency range, 0.1–1000 MHz; gain, 20 dB), a low-pass filter (SLP-850, Mini Circuit; cutoff frequency, 850 MHz), a variable attenuator (8494A for coarse tuning of 1 dB step attenuation, Agilent Technology, Palo Alto, CA; bandwidth, DC-4 GHz; maximum attenuation, −11 dB; and 2-3953-3Y for fine tuning of continuously attenuation, ARRA, NY; maximum attenuation, −3 dB; bandwidth 700 MHz–1.4 GHz), a power amplifier (A1000-1S-M, R&K, Japan; gain, 20 dB; maximum output power, 200 mW), and a phase shifter (6709, Sage Lab., Palo Alto, CA; frequency range, DC-1 GHz). To suppress standing waves in the transmission lines, fixed attenuators (3 dB) were used. The receiver coil, the phase tunable amplifier, and the excitation coil formed a positive feedback line. The feedback gain was controlled by a variable attenuator.

2.2. Frequency characteristics

The frequency characteristics of the active resonator system were investigated by using a network an-

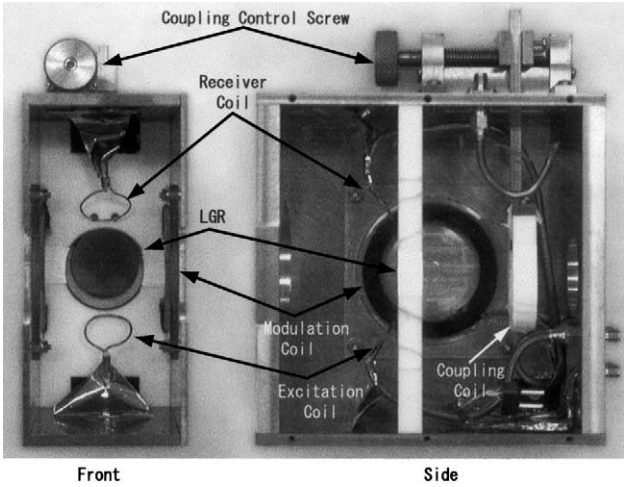

Fig. 2. Photograph of the shield case, including the LGR, the coupling coil, excitation and receiver coils, modulation coil, and control screw.

alyzer (8714C, Agilent Technology; frequency range, 300 kHz–3 GHz). A phantom that contained a nitroxide radical and physiological saline solution was located at the center of the LGR. Figs. 3a and b show reflections (linear scale) in the LGR without and with phantom vs. frequency, respectively (Qs without and with phantom, 900 and 55). When the feedback was applied with the phantom, the Q increased dramatically, as shown in Fig. 3c. The Q could be increased to 4000, which was higher than the Q of the LGR without the phantom. It was possible to tune the coupling between the resonator and the transmission line (50 Ω) in a matched condition by adjusting the feedback phase for any coupling distance. The Q of the resonator system increased with an increase in the coupling distance.

The transmission characteristic (logarithmic scale) between the excitation coil and receiver coil without and with phantom in the LGR is shown in Figs. 3d and e, respectively. The peak at the resonant frequency of the LGR showed that the RF power was transferred through the LGR. When the phantom was in the resonator, the peak height decreased and broadened. The feedback gain vs. frequency is shown in Fig. 3f. The

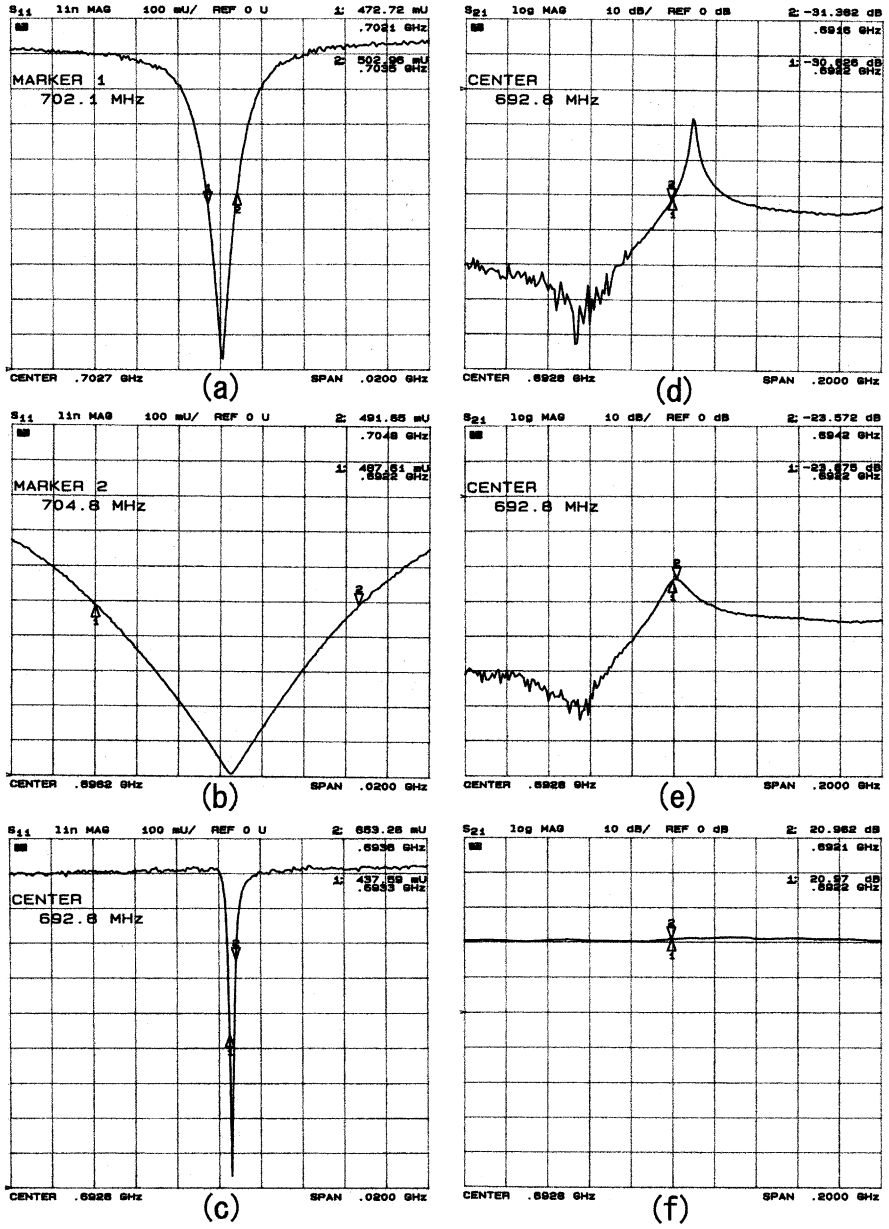

Fig. 3. Reflection (a–c) and transmission (d–f) characteristics of the active resonator system vs. frequency. Reflection in the LGR without phantom is shown in (a). Characteristics of the phantom-loaded LGR with and without feedback are shown in (c) and (b), respectively. The transmission characteristics between excitation coil and receiver coil with and without phantom are shown in (e) and (d), respectively. The feedback gain vs. frequency is shown in (f). Reflections (a–c) and transmissions (d–f) were presented on linear and logarithmic scales, respectively.

feedback gain was controlled at a constant value. To avoid oscillation, the total loop gain was controlled so as not to exceed 1. The direct coupling between the coupling coil and the receiver coil was measured at −35 dB at the resonant frequency of the LGR.

2.3. Signal and noise intensity of ESR spectra

The Q and ESR signal intensity of the phantom vs. coupling distance are shown in Fig. 4. The source power and the feedback gain were constant at 0.3 mW and 21 dB, respectively. The Q of the active resonator system increased with an increase in the coupling distance. The ESR signal intensity also increased; however, it became saturated in the area where the Q was high. The maximum ESR signal intensity of the active resonator system was seven times larger than it was under a no-feedback condition. The degree by which the signal intensity increased was smaller than that of Q.

Signal and noise intensities vs. coupling distance, shown in Fig. 5, both increased when the coupling distance was increased until saturation was reached. The experimental conditions were same as those described above. The noise intensity became saturated at a coupling distance that was shorter than for the signal intensity. The signal-to-noise ratio (SNR) vs. coupling distance of the active resonator system is shown in Fig. 6 (solid circles). The SNR observed for no-feedback was also plotted (open circle). Here the SNR was better for the same coupling distance (i.e., at the same Q); however, the best SNR using feedback was 50% higher than when there was no-feedback. The increase in the SNR was smaller than that of the signal intensity because the noise intensity also increased with the Q.

The signal intensity vs. feedback gain is shown in Fig. 7. In this experiment, the feedback gain was varied from 19 to 25 dB. The signal intensities were almost constant for different feedback gains when the coupling

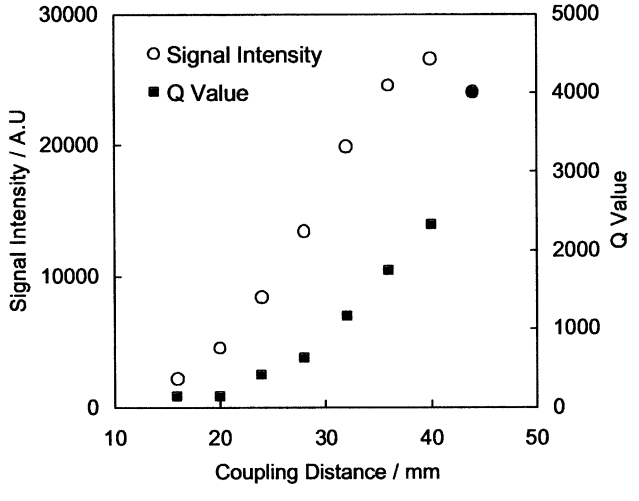

Fig. 4. Signal intensity and Q of the phantom vs. coupling distance. When the distance between the LGR and the coupling coil (coupling distance) was increased, the Q also increased. It was possible to tune the coupling by changing the phase of the feedback. The feedback gain and RF power were set at 21 dB and 0.3 mW, respectively. The signal intensity also increased with the coupling distance, although it became saturated and dropped in the area where the Q was high.

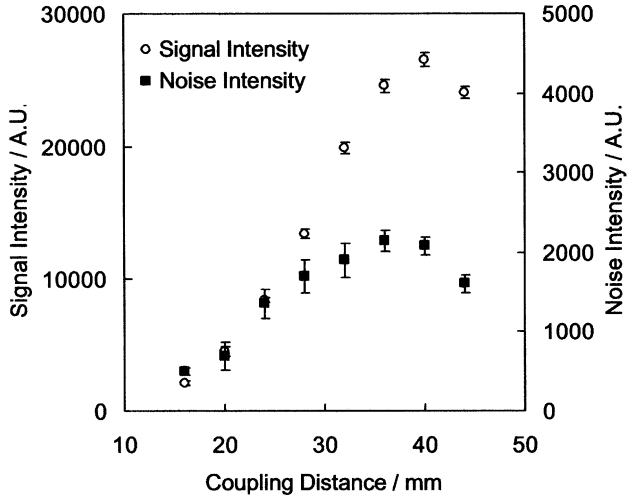

Fig. 5. Signal and noise intensities in ESR measurement of the phantom vs. coupling distance. The signal and noise intensities increased with an increase in coupling distance until saturation. When compared with the signal intensity, the noise intensity became saturated at a shorter coupling distance. The values were means ± standard deviation from five independent measurements.

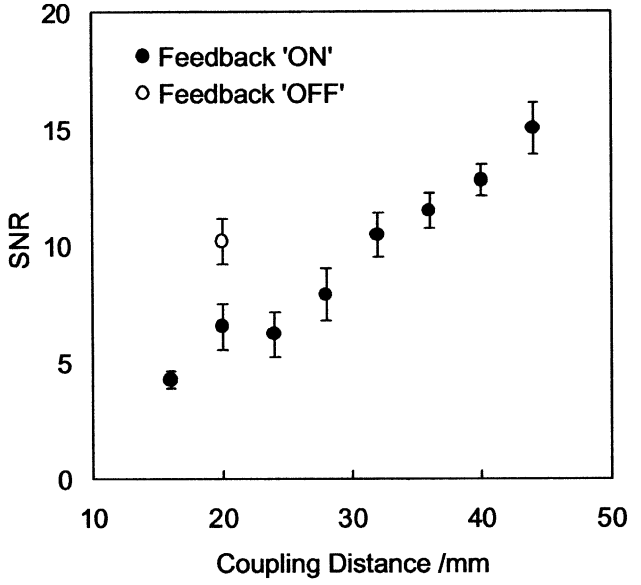

Fig. 6. SNR from ESR measurements of the phantom vs. coupling distance. Open and solid circles show the SNR without and with feedback, respectively. For the same coupling distance, the SNR without feedback was better; however, the best SNR, using feedback, was 50% higher than that at a no-feedback condition.

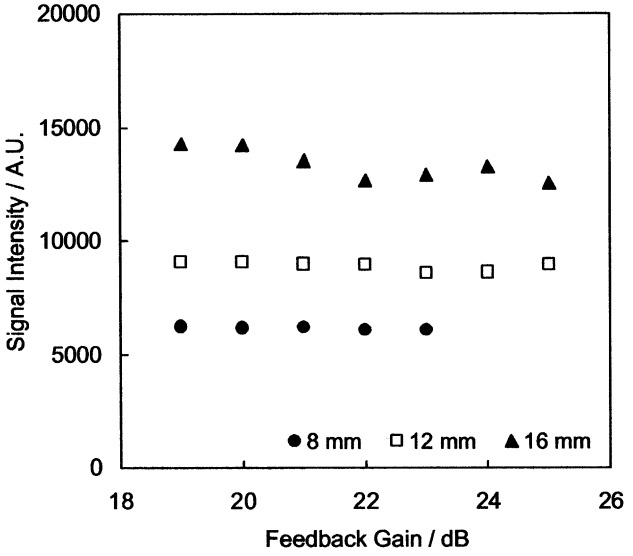

Fig. 7. Signal intensity from the phantom vs. feedback gain at coupling distances of 8, 12, and 16 mm. The signal intensity remained almost constant as the level of feedback gain was changed for a given coupling distance. Even when the feedback gain was changed, it was possible to adjust the coupling by changing the phase of the feedback.

distance was constant. Even when the feedback gain was changed, it was possible to tune the coupling by adjusting the phase of the feedback.

3. Discussion

It was verified that the active resonator system operates as anticipated; and the Q and ESR signal intensity both increased, the latter increasing with an increase in Q. However, in relative terms, the amount by which it increased was less than that of the Q. This may have occurred due to the direct coupling between the excitation coil, receiver coil or coupling coil. The energy stored in the line could reduce the actual filling factor of the active resonator system. However, because the direct coupling between the coupling coil and the receiver coil was −35 dB and the amplitude of the feedback amplifiers was less than 25 dB, the coupling coil, receiver coil, feedback amplifiers, and excitation coil could not perform as an effective amplifier system of source power.

The signal intensity became saturated and fell off in the area where the Q was high. It was proven that the amplifier used in the feedback loop had not saturated. B_1 in the resonator depends on Q, size of the resonator, the mode of B_1, and the frequency of the radiowave. When the wavelength is sufficiently longer than the diameter of the resonator, B_1 at the center of LGR is estimated by

$$B_1 = \mu_0/2r\sqrt{QW/\omega L}, \tag{2}$$

where the μ_0 is the permeability of free space, r is the radius of the loop, W is the applied power, ω is the angular velocity of the radiowave, and L is the inductance of the loop conductor which is a function of the radius and the axial length of the loop conductor. From this equation for a constant source power, B_1 increases when the Q increases. Therefore, in the active resonator system, an increased B_1 was applied to the sample when the Q was advanced. However, B_1 at the highest Q was under the level at which the ESR signal of the nitroxide radical was saturated. This was confirmed by using the conventional LGR system. The coupling distance in the area of high Q was most likely too great, which caused the phase to rotate considerably, reducing the signal intensity.

When the ESR signal intensity increased, so did the SNR. However, the increase in SNR was not proportional to either the Q or the signal intensity. There are three sources of noise in the active resonator system: the RF detector (such as the double balanced mixer, including the pre-amplifier before the mixer); the RF source; and noise generated by the amplifier that is used in the feedback circuit. Because the magnitude of the noise from the first source was constant, the SNR increased with an increase in signal intensity. However, the noise from the RF source tended to increase as the Q increased. Therefore, the SNR did not increase linearly with the increase in signal intensity. The noise from the third source was added in this active resonator system so the SNR at the same Q was worse than it was when there was no-feedback. However, the SNR did increase up to 50% in the area where the Q was high because the increase in signal intensity exceeded the noise added in this system.

If the feedback amplifiers re-supply all of the power dissipated by the losses in the resonator, the Q will become infinite, and the feedback circuit will oscillate. In this case, it is presumed that B_1 is maintained and ESR signal could be observed, even if the applied power is zero.

4. Experiment

4.1. ESR spectrometer

A 700 MHz-ESR spectrometer was constructed at our institute (already described in detail [5,6]). A commercially available resistive magnet (modified RE3X, JEOL, Japan) was used as the main magnet. The static magnetic field was scanned by controlling the current in a pair of field scan coils (Helmholtz type coil, Yonezawa Electric Wire, Japan). For lock-in detection, the magnetic field was modulated at a modulation frequency of 100 kHz by a pair of modulation coils. These coils (inner diameter, 46 mm; outer diameter, 68 mm; 40 turns; distance between coils, 66 mm) were driven by a power amplifier (4020, NF, Japan; gain, 46 dB) at 0.2 mT width. A synthesized oscil-

lator (MG3633A, Anritsu, Japan; frequency range, 10 kHz–2700 MHz) was used as an RF source for ESR excitation at 700 MHz. The RF circuit for ESR detection was constructed with a power amplifier (ZHL-2-12, Mini Circuit; frequency range, 10–1200 MHz; gain, 24); a VSWR bridge (BR-1N, Kuranishi, Japan; frequency range, 10–1300 MHz; insertion loss, 6.5 dB); a phase shifter (6602-3, Sage; frequency range, DC-2 GHz; minimum phase shift, 290°/GHz); a pre-amplifier (ZFL-1000LN, Mini Circuit; frequency range, 0.1–1000 MHz; gain, 20); and a double balanced mixer (M49, R&K; frequency range, 1–2000 MHz) for homodyne detection. The rectified signals were amplified by a low-noise amplifier (SA-230F5, NF; gain 46 dB; frequency range, 1 kHz–100 MHz; noise figure, 0.6 dB) and detected by a lock-in amplifier (5202, PARC, Princeton, NJ; frequency range, 1 mHz–1 MHz) at the magnetic field modulation frequency. An internal oscillator in the lock-in amplifier was used as the modulation signal source at 100 kHz. The instrumentation was controlled by a personal computer (PC9821Xa13, NEC, Japan) via a D/A converter (DAJ98, Canopus, Japan) and the spectral data were collected via an A/D converter (ADJ98, Canopus), also using the personal computer.

4.2. Phantom

Ten milliliters of a 1 mM solution of a nitroxide radical, 4-hydroxy-2,2,6,6-teramethylpipedin-1-oxyl (TEMPOL, Aldrich Chem., Milwaukee, WI), which had been dissolved in a physiological saline solution (a 0.9% sodium chloride aqueous solution), was placed in a sample tube (inner diameter, 20 mm; axial length, 31 mm) for use as a phantom.

4.3. ESR measurement

The phantom was placed at the center of the LGR, and then ESR measurements were made. The RF power was limited to 0.3 mW so that the amplifier used in the feedback circuit would not become saturated. The signal intensity was derived from the peak-to-peak height of the lowest component in a triplet spectrum. The noise intensity was defined as the product of the rms noise multiplied by $2\sqrt{2}$. The ESR conditions were: static magnetic field 25 mT; sweep width, 10 mT; sweep time, 2 s; time constant, 1 ms; and accumulation number, 16.

References

[1] W.N. Hardy, L.A. Whitehead, Split-ring resonator for use in magnetic resonance from 200 to 2000 MHz, Rev. Sci. Instrum. 52 (2) (1981) 213–216.
[2] W. Froncisz, J. Hyde, The loop-gap resonator: a new microwave lumped circuit ESR sample structure, J. Magn. Reson. 47 (1982) 515–521.
[3] M. Ono, T. Ogata, K. Hsieh, M. Suzuki, E. Yoshida, H. Kamada, L-band ESR spectrometer using a loop-gap resonator for in-vivo analysis, Chem. Lett. (1986) 491–494.
[4] H. Hirata, M. Ono, Resonance frequency estimation of bridged loop-gap resonator for magnetic resonance measurements, Rev. Sci. Instrum. 67 (1) (1996) 73–78.
[5] T. Sato, H. Yokoyama, H. Ohya, H. Kamada, A multilayered element resonator for CW-ESR and longitudinally detected ESR at radio frequency, Appl. Magn. Reson. 17 (1999) 119–131.
[6] H. Yokoyama, T. Sato, T. Ogata, H. Ohya, H. Kamada, Automatic coupling control of a loop-gap resonator by a variable capacitor attached coupling coil for EPR measurement, J. Magn. Reson. 149 (2001) 29–35.